SEMARAK ILMU PUBLISHING

Journal of Advanced Research in Fluid Mechanics and Thermal Sciences

Journal homepage:
https://semarakilmu.com.my/journals/index.php/fluid_mechanics_thermal_sciences/index
ISSN: 2289-7879

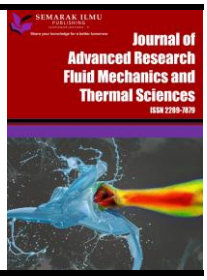

Radiation Effects on MHD Flow of Second Grade Fluid Through Porous Medium Past an Exponentially Stretching Sheet with Chemical Reaction

Abdelmgid Sidahmed[1], Faisal Salah[1,*]

[1] King Abdulaziz University, College of Science & Arts, Department of Mathematics, Rabigh 21911, Saudi Arabia

ARTICLE INFO

Article history:
Received 16 April 2022
Received in revised form 3 August 2022
Accepted 13 August 2022
Available online 9 September 2022

Keywords:
MHD stretching sheet; chemical reaction; second grade; Eckert number; thermal radiation

ABSTRACT

This article looked at the effects of electromagnetic force, chemical radiation, and thermal radiation on second-grade fluid passing through an exponentially stretched sheet with a heat sink and a porous medium. Using similarity transformations, the governing system of nonlinear partial differential equations has been converted into a system of ordinary differential equations. The Successive Linearization Method is then used to solve the system numerically. The main goal of this paper is to compare the results of solving the velocity, concentration and temperature equations in the presence of changes through SLM, introducing it as a precise and appropriate method for solving nonlinear differential equations. Graphs are used to display the numerical findings for the profiles of velocity, temperature, and concentration. The effects of various parameters are looked at and evaluated. The numerical values of the local Sherwood number, local Nusselt number, porosity, retardation number, and skin friction coefficient are presented and examined. The findings show that a wide range of variables significantly affect the fluid flow patterns. The reaction rate parameter had a significant impact on the concentration profiles, and as the reaction rate parameter grew, the boundary layer's concentration thickness reduced. The analysis's findings and the findings of previous studies were compared, and it was discovered that they were in excellent agreement.

1. Introduction

Many industrial operations, including hot rolling, chemical coating of flat plates, polymer extrusion, and heat exchange [1,2], heavily rely on chemical reactions. Since there might be a distant mass in the water or the air, pure water or air cannot exist naturally [3]. Because of this, certain mixtures may cause chemical changes in the constituent substances. By using a permeable plate and slope temperature, Sinha [4] explored the effects of chemical reaction on unsteady MHD free convective flow and found that raising the chemical reaction parameter causes the reaction rate to increase. The effects of radiation are studied by Chaudhary *et al.,* [5] and Ishak [6] for the MHD flow through an exponentially stretched sheet. As the Prandtl number rises, the rate of heat transfer rises as well, but it falls as the radiation and magnetic variables rise. As the radiation parameter is raised,

* *Corresponding author.*
E-mail address: frashed@kau.edu.sa

https://doi.org/10.37934/arfmts.99.2.116

the temperature increases. Research that combines the effects of radiation and chemical reactions on MHD flow is essential in many industries, including manufacturing [7-10]. The flow of the MHD boundary layer over an exponentially stretched sheet under the influence of chemical reaction and radiation was explored [11-15], and the concentration of the boundary layer increased when the reaction rate parameter was increased. The unsteady energy and mass transport of magnetohydrodynamics (MHD) second grade nanofuid via an exponentially extending surface with Dufour and Soret effects are investigated by Siddique *et al.,* [16]. The findings show that the temperature of the fluid grew in direct proportion to the thermophoresis motion, buoyancy ratio, and Brownian motion parameters. The chemical reaction and variable viscosity effects on the flow and mass transfer of a non-Newtonian visco-elastic second grade fluid past a stretching surface embedded in a porous medium were studied by Mahmoud [17]. He found that the local Sherwood number increases with increasing the visco-elastic parameter or the Shemidt number or the viscosity parameter or the destructive chemical reaction parameter and decreases as the slip parameter or the Darcy parameter or the absolute values of the generative chemical reaction parameter increase. The governing equation for the second grade fluid is of fourth order in general. When higher-order nonlinearities are neglected, the order of equation in the second grade fluid is reduced [18,19]. Some of these problems are solved using traditional numerical approaches such as the finite difference method, shooting method, Keller box method [20], Runge-Kutta and artificial neural networks (ANNs) [21-26]. A new method called the Successive Linearization Method has just been proposed in various papers (SLM). This approach has the following key features, which are justified: It is a strong approach to solving these types of problems since it converts the original linear differential equation into a system of linear algebraic equations. This method has been applied successfully to a wide range of nonlinear problems in science and engineering, including [27-30]. As a result, all of these successful applications attest to the SLM's usefulness, validity, accuracy, and flexibility.

As a result, the goal of this research is to expand ref [11] and ref [31] findings to a broader problem, such as the effect of second grade fluid dissipation and chemical reaction on MHD in porous medium. The effects of various flow parameters encountered in the governing equations are shown visually and tabulated in this work. The problem is numerically addressed using the SLM approach, which is more computationally efficient. The pertinent results are displayed graphically and discussed quantitatively.

The rest of the paper is organized as follows. The governing system of nonlinear partial differential equations has been converted into a system of ordinary differential equations in Section 2. Section 3 deals with the application of SLM to solve our problem. Finally, some numerical results along with a discussion on them are given in Section 4.

2. Mathematical Formulation

Consider two-dimensional free convective heat and mass transport down a semi-infinite vertical plate embedded in a doubly stratified, electrically conducting second grade fluid that is stable, laminar, and incompressible. Select a coordinate system with the x-axis parallel to the vertical plate and the y-axis perpendicular to the plate. Figure 1 illustrates the physical model and coordinate system. A uniform magnetic field of the same magnitude is applied to the plate in a normal direction. Because the magnetic Reynolds number is minimal, the induced magnetic field can be ignored in comparison to the applied magnetic field.

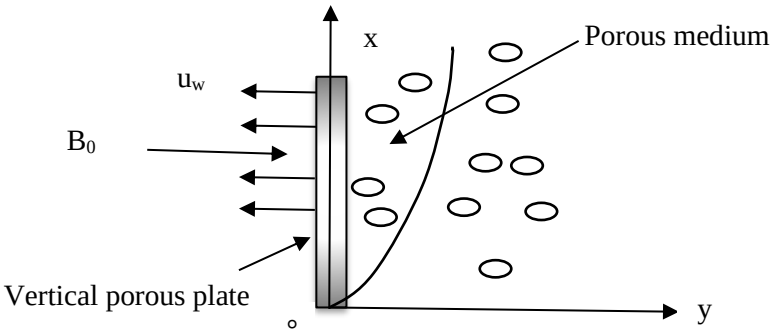

Fig. 1. Flow geometry

This research also made assumptions $T = T_w = T_\infty + T_0 e^{\frac{x}{2L}}$, $\mathrm{C} = \mathrm{C}_w = \mathrm{C}_\infty + \mathrm{C}_0 e^{\frac{x}{2L}}$ where $T_w > T_\infty$ and $C_w > C_\infty$. The governing equations for the second grade fluid as given by Fetecau *et al.,* [33] and Hayat *et al.,* [34] using the Boussinesq and boundary layer approximations as described by Sparrow and Abraham *et al.,* [35] are given by

$$\frac{\partial u}{\partial x} + \frac{\partial v}{\partial y} = 0, \tag{1}$$

$$u\frac{\partial u}{\partial x} + v\frac{\partial u}{\partial y} = \upsilon\frac{\partial^2 u}{\partial y^2} + \upsilon\lambda_1\left(u\frac{\partial^3 u}{\partial x \partial y^2} - \frac{\partial u}{\partial x}\frac{\partial^2 u}{\partial y^2} + v\frac{\partial^3 u}{\partial y^3} - \frac{\partial u}{\partial y}\frac{\partial^2 v}{\partial y^2}\right) - \left(\frac{\upsilon}{k} + \frac{\sigma}{\rho}B_0^2\right)u + g\beta_c\left(C - C_\infty\right), \tag{2}$$

$$u\frac{\partial T}{\partial x} + v\frac{\partial T}{\partial y} = \alpha\frac{\partial^2 T}{\partial y^2} - \frac{1}{\rho c_p}\frac{\partial q_r}{\partial y} + \frac{Q}{\rho c_p}\left(T - T_\infty\right), \tag{3}$$

$$u\frac{\partial C}{\partial x} + v\frac{\partial C}{\partial y} = D\frac{\partial^2 C}{\partial y^2} - k_1(x)\left(C - C_\infty\right). \tag{4}$$

The temperature, velocity, and concentration profiles have corresponding boundary conditions.

$$\begin{aligned} &u = U_w = \mathrm{U}_0 e^{\frac{x}{L}}, v = 0, \\ &T = T_w = T_\infty + T_0 e^{\frac{x}{2L}}, \\ &\mathrm{C} = \mathrm{C}_w = \mathrm{C}_\infty + \mathrm{C}_0 e^{\frac{x}{2L}} \quad at \quad y = 0. \end{aligned} \tag{5}$$

$$u \to 0, T \to T_\infty, \ \mathrm{C} \to \mathrm{C}_\infty \quad at \quad y \to \infty. \tag{6}$$

The continuity Eq. (1) is satisfied by introducing the stream function ψ such that

$$u = \frac{\partial \psi}{\partial y}, v = -\frac{\partial \psi}{\partial x}. \tag{7}$$

2.1 Similarity Conversion

A similarity transformation is used to turn the set of partial differential equations that govern this system into ordinary differential equations. The following non-dimensional variables developed by Mukhopadhyay [36] are used to simplify the resulting equations. For radiation, we have used the Rosseland approximation.

$$\begin{aligned}
&\eta = y\sqrt{\frac{U_0}{2\upsilon L}}\,e^{x/2L},\\
&u = U_0 e^{x/L} f'(\eta),\\
&v = -\sqrt{\frac{\upsilon U_0}{2L}}e^{x/2L}\left[f(\eta)+\eta f'(\eta)\right],\\
&T = T_\infty + T_0\, e^{x/2L}\theta(\eta),\\
&C = C_\infty + C_0\, e^{x/2L}\phi((\eta)),\\
&B = B_0\, e^{x/2L}.
\end{aligned} \tag{8}$$

Substituting (7) and (8) in (2)–(6), it is found that a similarity exists and hence we obtain

$$f''' - 2f'^2 + ff'' + \beta_1(3f''^2 + 2ff''' - ff''') - \left(\frac{1}{K_p} + M\right)f' + \lambda\phi(\eta) = 0, \tag{9}$$

$$\left(1+\frac{4}{3}R\right)\theta'' + P_r(f\theta' - f'\theta + S\theta) = 0, \tag{10}$$

$$\phi'' + S_c(f\phi' - f'\phi - \gamma\phi) = 0, \tag{11}$$

where

$$\beta_1 = \frac{\lambda_1 U_0 e^{x/L}}{2L},\ M = \frac{2\sigma B_0^2 L}{U_0\rho e^{x/L}},\ \frac{1}{K_p} = \frac{2\upsilon L}{U_0 K_p' e^{x/L}},\ \ \lambda = \frac{2LC_0 g\beta_c}{U_0 e^{3x/L}}.$$

where primes denote differentiation with respect to similarity variables. Boundary conditions (5) and (6) in terms of f , g , θ and ϕ become

$$\begin{aligned}
&f(0) = 0,\\
&f'(0) = 1,\\
&f'(\infty) = 0,\\
&\theta(0) = 1,\\
&\phi(0) = 1,
\end{aligned} \tag{12}$$

$$f'(\eta) = 0, \theta(\eta) = 0, \phi(\eta) = 0 \ \ as \ \ \eta \to \infty.$$

Physical Quantities of interest,
The local skin friction coefficient C_f is defined as

$$\frac{1}{\sqrt{2}} C_f \sqrt{R_e} = f''(0). \tag{13}$$

The heat and mass transfers from the plate, respectively, are given by

$$\begin{gathered} q_w = -k\left(\frac{\partial T}{\partial y}\right)_{y=0}, \; q_m = -D\left(\frac{\partial C}{\partial y}\right)_{y=0}, \\ \frac{N_u}{\sqrt{R_e}} = -\theta'(0), \; \frac{S_h}{\sqrt{R_e}} = -\phi'(0), \quad \text{Where } R_e = \frac{U_w}{\nu}. \end{gathered} \tag{14}$$

3. Numerical analysis

The transformed system of ordinary differential Eq. (9) – (11) is numerically solved using the boundary conditions (12) and utilizes the SLM.
For SLM solution we select the initial guesses functions $f(\eta)$, $\theta(\eta)$ and $\phi(\eta)$ in the form

$$f(\eta) = f_i(\eta) + \sum_{m=0}^{i-1} F_m(\eta) \;,\; \theta(\eta) = \theta_i(\eta) + \sum_{m=0}^{i-1} \theta_m(\eta) \text{ and } \phi(\eta) = \phi_i(\eta) + \sum_{m=0}^{i-1} \phi_m(\eta). \tag{15}$$

Here the three functions $f_i(\eta)$, $\theta_i(\eta)$ and $\phi_i(\eta)$ are representative unknown functions. $F_m(\eta)$, $m \geq 1$, $\theta_m(\eta)$, $\phi(\eta)$ $m \geq 1$ are successive approximation which are obtained by recursively solving the linear part of the equation that results from substituting Eq. (15) in the governing equations.

The mean idea of SLM that the assumption of unknown function $f_i(\eta)$, $\theta_i(\eta)$ and $\phi_i(\eta)$ are very small when i becomes larger, therefore, the nonlinear terms in $f_i(\eta)$, $\theta_i(\eta)$ and $\phi_i(\eta)$ and their derivatives are considered to be smaller and thus neglected. The intimal guess functions $F_o(\eta)$, $\theta_o(\eta)$ and $\phi_o(\eta)$ which are selected to satisfy the boundary conditions

$$\begin{gathered} F_0(\eta) = 0 \,,\, F_0'(\eta) = 1 \quad at \quad \eta = 0, \\ F_0'(\eta) \to 0 \,,\, F_0''(\eta) \to 0 \quad at \quad \eta \to \infty, \\ \theta_o(0) = 1, \;\; \theta_o(\infty) \to 0, \\ \phi_o(0) = 1, \;\; \phi_o(\infty) \to 0. \end{gathered} \tag{16}$$

which are taken to be in the form

$$F_0(\eta) = \left(1 - e^{-\eta}\right) \quad \theta_0(\eta) = e^{-\eta} \text{ and } \quad \phi_0(\eta) = e^{-\eta} \tag{17}$$

We arrive at

$$\begin{aligned} &a_1 D^4 + a_2 D^3 + a_3 D^2 + a_4 D + a_5 I + \lambda \phi_i = r_1, \\ &D^2 + b_1 D + b_2 I + a_6 D + a_7 I = r_2, \\ &c_1 D^2 + c_2 D + c_3 I + a_8 D + a_9 I = r_3. \end{aligned} \tag{18}$$

where

$$\begin{aligned} &a_1 = -\beta_1 \sum f_n,\ a_2 = 1 + 2\beta_1 \sum f_n{}',\ a_3 = \sum f_n + 6\beta_1 \sum f_n{}'',\ a_4 = -4\sum f_n{}' + 2\sum f_n{}''' - \left(\frac{1}{K_p} - M\right), \\ &a_5 = \sum f_n{}'' - \beta_1 \sum f_n{}'''',\ a_6 = -S_c \sum \phi_n,\ a_7 = S_c \sum \phi_n{}', \\ &a_8 = -P_r \sum \theta_n, a_9 = P_r \sum \theta_n{}'. \end{aligned} \tag{9}$$

$$b_1 = S_c \sum f_n,\ b_2 = -S_c \left(\gamma + \sum f_n{}'\right) \tag{20}$$

$$c_1 = \left(1 + \frac{4}{3}R\right),\ c_2 = P_r + 2\sum f_n, c_3 = P_r \left(S - \sum f_n{}'\right) \tag{21}$$

$$\begin{aligned} r_1 = &-\sum f_n''' + 2\left(\sum f_n'\right)^2 - \sum f_n \sum f_n'' - 3\beta_1 \left(\sum f_n''\right)^2 - 2\beta_1 \sum f_n' \sum f_n''' + \beta_1 \sum f_n \sum f_n'''' \\ &+ \left(\frac{1}{K_p} - M\right) \sum f_n' - \lambda \sum \phi_n, \\ r_2 = &-\sum \phi_n'' - S_c \left(\sum f_n \sum \phi_n' - \gamma \sum \phi_n - \sum f_n' \sum \phi_n\right), \\ r_3 = &-\left(1 + \frac{4}{3}R\right) \sum \theta_n'' - P_r \sum f_n \sum \theta_n' + P_r \sum f_n' \sum \theta_n - SP_r \sum \theta_n. \end{aligned} \tag{22}$$

Eq. (18) can be written as a system of linear equations

$$\begin{aligned} &AX = B \\ &A = \begin{bmatrix} A_{11} & A_{12} & 0 \\ A_{21} & A_{22} & 0 \\ A_{31} & 0 & A_{33} \end{bmatrix},\ X = \begin{bmatrix} f \\ \phi \\ \theta \end{bmatrix},\ B = \begin{bmatrix} r_1 \\ r_2 \\ r_3 \end{bmatrix}. \end{aligned} \tag{23}$$

where

$$
\begin{aligned}
A_{11} &= a_1 D^4 + a_2 D^3 + a_3 D^2 + a_4 D + a_5 I \\
A_{12} &= \lambda I \\
A_{21} &= a_6 D + a_7 I \\
A_{22} &= D^2 + b_1 D + b_2 I \\
A_{31} &= a_8 D + a_9 I \\
A_{33} &= c_1 D^2 + c_2 D + c_3 I
\end{aligned}
\tag{24}
$$

4. Results and Discussion

4.1 Validation of Study

Table 1 illustrates the Nusselt number $-\theta'(0)$ values for various radiation parameters, while the remainder of the parameters are set to zero, where $P_r = 1, K = 100$. The table compares the results obtained with those of Reddy *et al.,* [31] and Swain *et al.,* [37], and it shows that the results agree with each other. Table 2, 3 and 4 show the values of Skin Friction Coefficient, Local Nusselt Number and Local Sherwood Number, respectively, for various values of the parameters involved. The table compares the results obtained with those of Khalili *et al.,* [32], and it shows that the results are in excellent agreement.

Table 1
Nusselt number $-\theta'(0)$

M	Pr	R	K	β_1	$-\theta'(0)$Ref. [31]	$-\theta'(0)$Ref. [37]	$-\theta'(0)Present$
0	1	1	100	0	0.5245	0.53119	0.530097611
0	1	0	100	0	0.947214	0.9547	0.953661340

Table 2
Values of Skin Friction Coefficient in comparison to the previous study ref. [32]

M	Pr	S	Sc	R	γ	K	β_1	λ	$\lvert f''(0)\rvert$Ref.[32]	$\lvert f''(0)\rvert present$
0	1	-0.5	0.22	1	1	0	0	0	1.281933	1.281808
2	5	-0.2	0.22	1	1	0	0	0	1.912633	1.912620
2	1	-0.5	0.22	1	1	0	0	0	1.912633	1.912620
2	1	-0.5	0.22	2	1	0	0	0	1.912633	1.912620

Table 3
Values of Local Nusselt Number in comparison to the previous study ref. [32]

M	Pr	S	Sc	R	γ	K	β_1	λ	$-\theta'(0)$Ref.[32]	$-\theta'(0)present$
0	1	-0.2	0.22	1	1	0	0	0	0.753584	0.753562
2	5	-0.2	0.22	1	1	0	0	0	1.555244	1.555223
2	1	-0.5	0.22	1	1	0	0	0	0.690717	0.690708
2	1	-0.5	0.22	2	1	0	0	0	0.526667	0.526591

Table 4
Values of Local Sherwood Number in comparison to the previous study ref [32]

M	Pr	S	Sc	R	γ	K	β_1	λ	$-\phi'(0)$Ref.[32]	$-\phi'(0)present$
0	1	-0.2	0.22	1	1	0	0	0	0.621791	0.621762
2	5	-0.2	0.22	1	1	0	0	0	0.586786	0.586776
2	1	-0.5	0.22	1	1	0	0	0	0.586786	0.586776
2	1	-0.5	0.22	2	1	0	0	0	0.586786	0.586776

4.2 Results

In the current study, thermal radiation in the presence of an even source and sink of heat is considered along with the chemical reaction flow of a second-grade incompressible electrically conducting fluid past an exponentially extending sheet via a porous medium. The examination of mass transfer has also been discussed in this paper. The purpose of the discussion that follows is to emphasize the effects of thermal radiation, medium permeability, and plate temperature on flow phenomena. In addition, the values of Skin Friction Coefficient, Local Nusselt Number and Local Sherwood Number for various values of parameters are shown in Table 5.

Table 5
Skin Friction Coefficient, Local Nusselt Number and Local Sherwood Number for various values of parameters involved using SLM

M	Pr	S	Sc	R	γ	K	β_1	λ	$\lvert f''(0)\rvert$	$-\theta'(0)$	$-\phi'(0)$
0	1	- 0.5	0.22	1	1	100	0.01	0.01	1.264956945	0.754579457	0.622333352
1									1.605792119	0.716510911	0.600823469
2									1.884181763	0.691956181	0.587442083
4									2.342832412	0.660223811	0.570534662
2	1	-0.2	0.22	1	1	100	0.01	0.01	1.888265436	0.555210203	0.587084622
	2								1.888265436	0.874525710	0.587084622
	3								1.888265436	1.133692117	0.587084622
	5								1.888265436	1.557433310	0.587084622
2	1	-0.3	0.22	1	1	100	0.01	0.01	1.888265436	0.606432814	0.587084622
		-0.5							1.888265436	0.691301659	0.587084622
		-1.0							1.888265436	0.854929536	0.587084622
		-1.2							1.888265436	0.909781830	0.587084622
2	1	-0.5	0.22	1	1	100	0.01	0.01	1.888265437	0.691301659	0.587084622
			0.30						1.888062921	0.691382439	0.699296434
			0.40						1.887862156	0.691455896	0.822440793
			0.62						1.887536560	0.691561733	1.052340488
2	1	-0.5	0.22	0	1	100	0.01	0.01	1.888265437	1.145572765	0.587084622
				1					1.888265436	0.691301659	0.587084622
				2					1.888265436	0.526966053	0.587084622
				3					1.888265436	0.437539299	0.587084622
2	1	-0.5	0.22	1	1	100	0.01	0.01	1.888265437	0.691301659	0.587084622
					2				1.887930535	0.691434558	0.766708072
					3				1.887709884	0.691510878	0.906858526
					5				1.887410673	0.691601443	1.131928276
2	1	-0.5	0.22	1	1	0.5	0.01	0.01	2.344189279	0.659866944	0.570344227
						1.0			2.127432437	0.673688693	0.577661254
						10			1.911259318	0.689485423	0.586107108
						100			1.888265436	0.691301659	0.587084622
2	1	-0.5	0.22	1	1	100	0.00	0.01	1.919420462	0.689843511	0.586305402
							0.02		1.858377579	0.692742546	0.587855372
							0.04		1.802097024	0.695573767	0.589372068
							0.06		1.750025311	0.698339566	0.590856655
2	1	-0.5	0.22	1	1	100	0.01	0.01	1.888265437	0.691301659	0.587084622
								0.09	1.918279896	0.712462615	0.553327940
								0.12	1.917794719	0.816848863	0.494409757
								0.15	1.918243796	0.917665744	0.487628890

The relationship between velocity and significant magnetic field levels is shown in Figure 2(a). It has been shown that boosting M lowers the velocity profile. As M rises, a resistive force known as the Lorentz force, which is akin to a drag force, is produced. The velocity intensity slows down as a result of the Lorentz force. Figure 2(b) illustrates how the magnetic field affects temperature profiles. Figure 2(b) depicts the formation of a magnetic field on the temperature profile. Due to the Lorentz force's connection to this magnetic field, an increase in temperature results from the Lorentz force's involvement in the characteristics of this most expansive magnet field. Dimensionless concentration is shown to be impacted by the magnetic field M in Figure 2(c). It is believed that the concentration profile will rise as M levels rise.

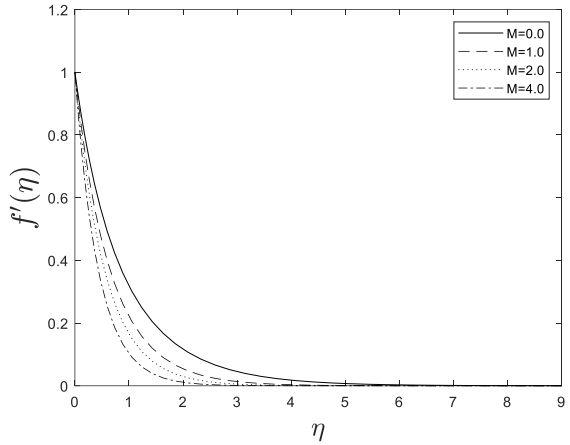

Fig. 2(a). Different values of M on the velocity profile

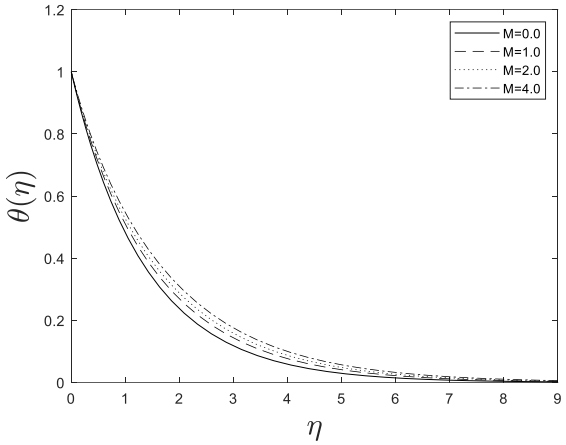

Fig. 2(b). Different values of M on the temperature profile

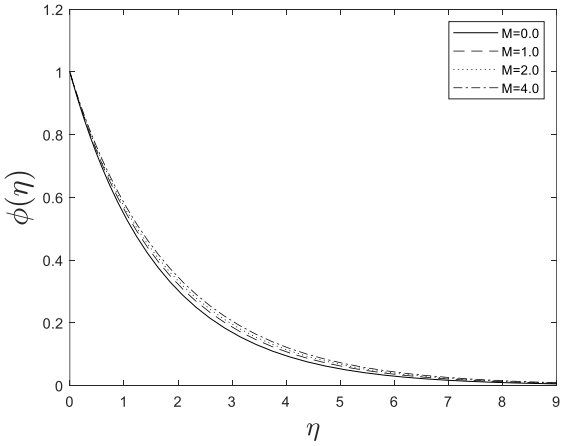

Fig. 2(c). Different values of M on the concentration profile

According to the graph in Figure 3(a), the fluid flow resistive force decreases as the porosity parameter increases, meaning that the fluid flow velocity rises as well. The impact of the porosity parameter K_p on temperature profiles is depicted in Figure 3(b). The temperature profile is shown to be decreasing in Figure 3(b) as a result of an increase in the porosity parameter. Figure 3(c) displays how the porosity parameter K_p affects dimensionless concentration. It is demonstrated that as the porosity parameter K_p increases, the concentration profile declines.

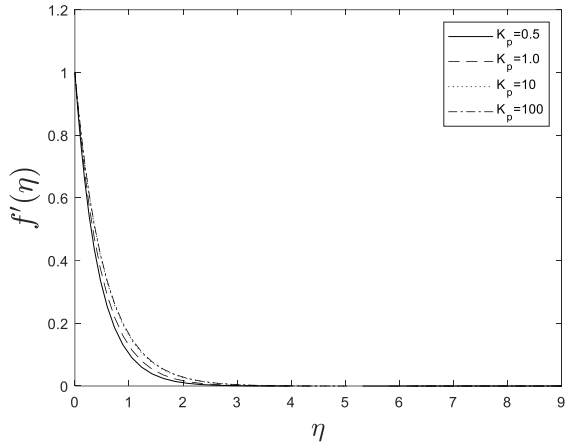

Fig. 3(a). Different values of permeability K_p on the velocity profile

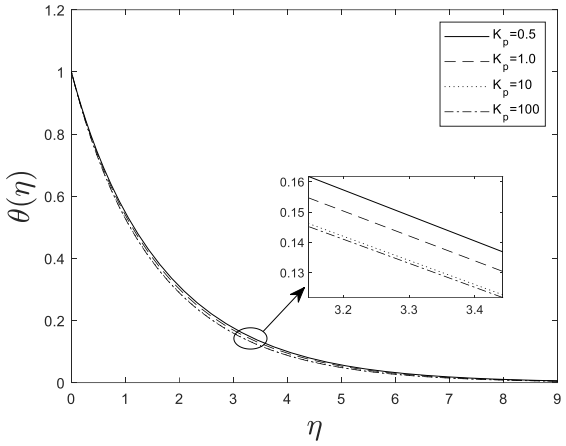

Fig. 3(b). Different values of permeability K_p on the temperature profile

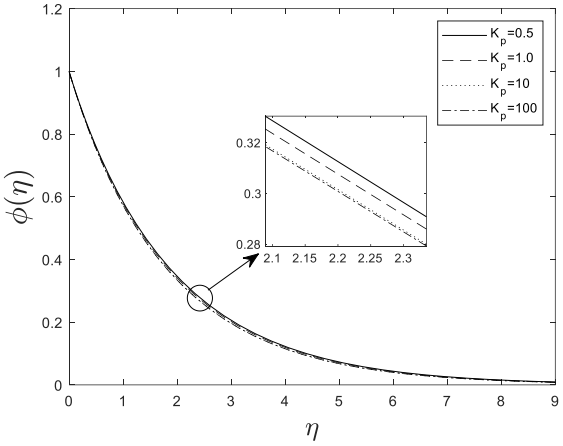

Fig. 3(c). Different values of permeability K_p on the concentration profile

Figure 4(a) depicts how radiation R affects the temperature profile. As the radiation R increases, the temperature rises. This happens as a result of a decrease in the rate of heat transmission over the surface area. Figure 4(b) illustrates how the Prandtl number affects the temperature profile. It's important to keep in mind that decreasing the Prandtl number results in a thinner thermal boundary layer.

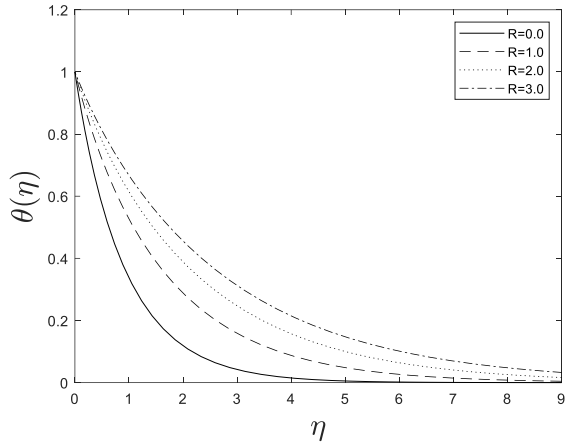

Fig. 4(a). Different values of thermal radiation R on the temperature profile

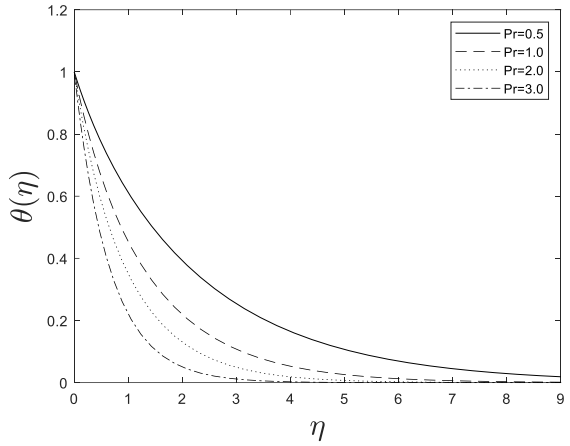

Fig. 4(b). Different values of Prandtl number P_r on the temperature profile

In Figure 5, the impact of the Schmidt number S_c on dimensionless concentration is depicted. A decrease in concentration is seen when the Schmidt number S_c rises.

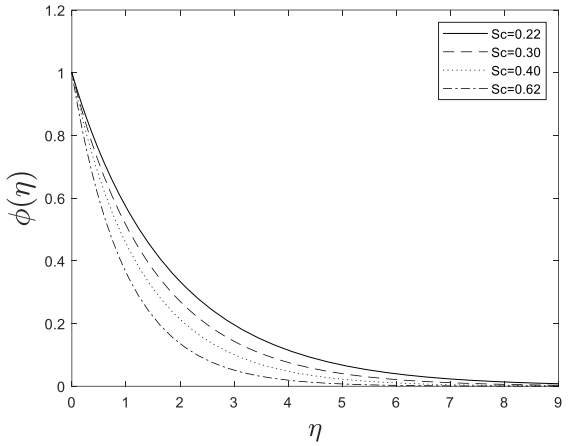

Fig. 5. Different values of Schmidt number S_c on the concentration profile

Figure 6 shows the effect of the chemical reaction γ on the concentration profile. The concentration decreases with an increase in the chemical reaction's γ.

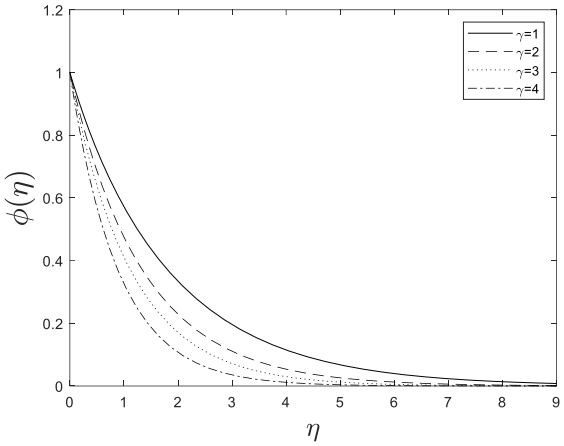

Fig. 6. Different values of chemical reaction γ on the concentration profile

Figure 7 illustrates how the source parameter (sink) S affects the temperature profile. The temperature profile seems to be improving when source parameter S is increased.

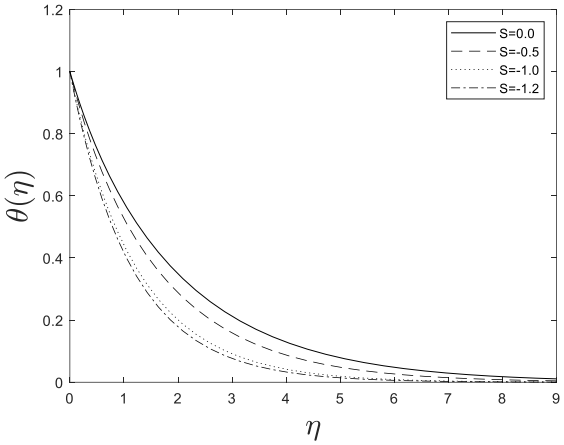

Fig. 7. Different values of source parameter (sink) S on the temperature profile

The effects of the retardation time constant β_1 on the velocity function f' are seen in Figure 8a. When β_1 is increased, the fluid flow and the thickness of the boundary layer are both improved. The effects of β_1 on θ and ϕ are depicted in Figure 8b and Figure 8c, respectively. The temperature and concentration profiles are observed to decline as β_1 increases. When various values of the parameters involved are studied, Table 2 displays the absolute values of the skin friction coefficient $f''(0)$, the values of the local Nusselt number $-\theta'(0)$, and the local Sherwood number $-\phi'(0)$.

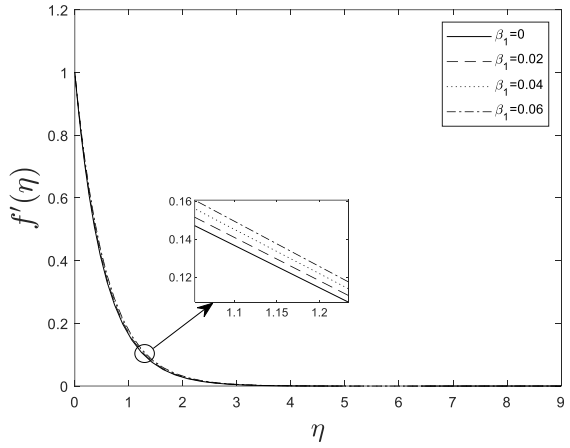

Fig. 8(a). Different values of β_1 on the velocity profile

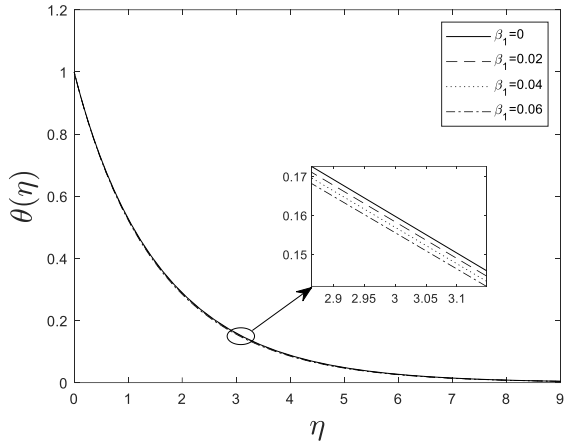

Fig. 8(b). Different values of β_1 on the temperature profile

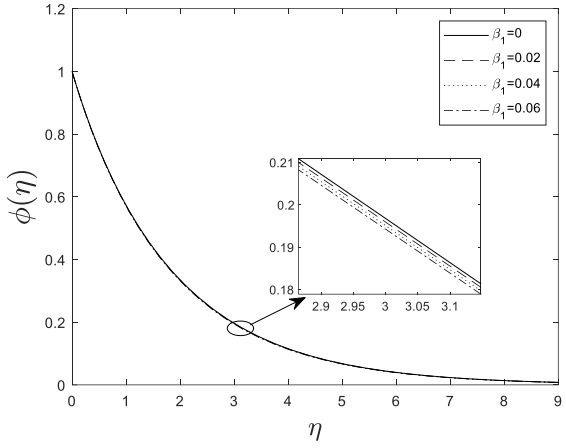

Fig. 8(c). Different values of β_1 on the concentration profile

5. Concluding Remarks

This study investigates the impact of chemical processes on the radiative MHD flow of Oldroyd-B fluid across a stretching sheet in porous material in the presence of viscous dissipation. The formulae for the velocity, temperature, and concentration distributions, which are the equations governing the flow, are numerically solved using the SLM method. Tables show how the Sherwood number, the Nusselt number, and skin friction are impacted by various governing parameters. Temperature and nanoparticle concentration rise as magnetic field levels rise, but dimensionless velocity decreases. When the porosity parameter K_p rises, indicating an increase in velocity profile, while concentration and temperature fields show the opposite trend. When the Prandtl number increases, the temperature and thickness of the thermal boundary layer decrease. The Nusselt number increases as β_1 and P_r increase, and the Schmidt number and the chemical reaction parameter with higher values reduce the nanoparticle concentration.

References

[1] Ibrahim, S. Y., and Oluwole D. Makinde. "Chemically reacting Magnetohydrodynamics (MHD) boundary layer flow of heat and mass transfer past a low-heat-resistant sheet moving vertically downwards." (2011). https://doi.org/10.5897/SRE2022.6751

[2] Ganesh, Ganugapati Raghavendra, and Wuriti Sridhar. "Effect of Chemical Reaction towards MHD Marginal Layer Movement of Casson Nanofluid through Porous Media above a Moving Plate with an Adaptable Thickness." *Pertanika Journal of Science & Technology* 30, no. 1 (2022). https://doi.org/10.47836/pjst.30.1.26

[3] Muhaimin, I., Ramasamy Kandasamy, I. Hashim, and Azme B. Khamis. "On the effect of chemical reaction, heat and mass transfer on nonlinear MHD boundary layer past a porous shrinking sheet with suction." *Theoretical and Applied Mechanics* 36, no. 2 (2009): 101-117. https://doi.org/10.2298/TAM0902101M

[4] Sinha, S. "Effect of chemical reaction on an unsteady MHD free convective flow past a porous plate with ramped temperature." In *Proceedings of International Conference on Frontier in Mathematics*. 2015.

[5] Chaudhary, Santosh, Sawai Singh, and Susheela Chaudhary. "Thermal radiation effects on MHD boundary layer flow over an exponentially stretching surface." *Applied Mathematics* 6, no. 02 (2015): 295. https://doi.org/10.4236/am.2015.62027

[6] Ishak, Anuar. "MHD boundary layer flow due to an exponentially stretching sheet with radiation effect." *Sains Malaysiana* 40, no. 4 (2011): 391-395.

[7] Lv, Yu-Pei, Naila Shaheen, Muhammad Ramzan, M. Mursaleen, Kottakkaran Sooppy Nisar, and M. Y. Malik. "Chemical reaction and thermal radiation impact on a nanofluid flow in a rotating channel with Hall current." *Scientific Reports* 11, no. 1 (2021): 1-17. https://doi.org/10.1038/s41598-021-99214-y

[8] Punith Gowda, R. J., R. Naveen Kumar, A. M. Jyothi, B. C. Prasannakumara, and Kottakkaran Sooppy Nisar. "KKL correlation for simulation of nanofluid flow over a stretching sheet considering magnetic dipole and chemical reaction." *ZAMM-Journal of Applied Mathematics and Mechanics/Zeitschrift für Angewandte Mathematik und Mechanik* 101, no. 11 (2021): e202000372. https://doi.org/10.1002/zamm.202000372

[9] Haq, Sami Ul, Syed Inayat Ali Shah, Kottakkaran Sooppy Nisar, Saeed Ullah Jan, and Ilyas Khan. "Convection heat mass transfer and MHD flow over a vertical plate with chemical reaction, arbitrary shear stress and exponential heating." *Scientific Reports* 11, no. 1 (2021): 1-11. https://doi.org/10.1038/s41598-021-81615-8

[10] Khan, Ansab Azam, Khairy Zaimi, Suliadi Firdaus Sufahani, and Mohammad Ferdows. "MHD flow and heat transfer of double stratified micropolar fluid over a vertical permeable shrinking/stretching sheet with chemical reaction and heat source." *Journal of Advanced Research in Applied Sciences and Engineering Technology* 21, no. 1 (2020): 1-14. https://doi.org/10.37934/araset.21.1.114

[11] Seini, Y. I., and O. D. Makinde. "MHD boundary layer flow due to exponential stretching surface with radiation and chemical reaction." *Mathematical Problems in Engineering* 2013 (2013). https://doi.org/10.1155/2013/163614

[12] Agarwal, Vandana, Bhupander Singh, and Kottakkaran Sooppy Nisar. "Numerical analysis of heat transfer in magnetohydrodynamic micropolar jeffery fluid flow through porous medium over a stretching sheet with thermal radiation." *Journal of Thermal Analysis and Calorimetry* (2022): 1-23. https://doi.org/10.1007/s10973-022-11224-8

[13] Bakar, Fairul Naim Abu, and Siti Khuzaimah Soid. "MHD Stagnation-Point Flow and Heat Transfer Over an Exponentially Stretching/Shrinking Vertical Sheet in a Micropolar Fluid with a Buoyancy Effect." *Journal of Advanced Research in Numerical Heat Transfer* 8, no. 1 (2022): 50-55.

[14] Dadheech, Praveen Kumar, Priyanka Agrawal, Anil Sharma, Kottakkaran Sooppy Nisar, and Sunil Dutt Purohit. "Marangoni convection flow of γ–Al2O3 nanofluids past a porous stretching surface with thermal radiation effect in the presence of an inclined magnetic field." *Heat Transfer* 51, no. 1 (2022): 534-550. https://doi.org/10.1002/htj.22318

[15] Mahat, Rahimah, Muhammad Saqib, Imran Ulah, Sharidan Shafie, and Sharena Mohamad Isa. "MHD Mixed Convection of Viscoelastic Nanofluid Flow due to Constant Heat Flux." *Journal of Advanced Research in Numerical Heat Transfer* 9, no. 1 (2022): 19-25.

[16] Siddique, Imran, Muhammad Nadeem, Jan Awrejcewicz, and Witold Pawłowski. "Soret and Dufour effects on unsteady MHD second-grade nanofluid flow across an exponentially stretching surface." *Scientific Reports* 12, no. 1 (2022): 1-14. https://doi.org/10.1038/s41598-022-16173-8

[17] Mahmoud, Mostafa AA. "Chemical reaction and variable viscosity effects on flow and mass transfer of a non-Newtonian visco-elastic fluid past a stretching surface embedded in a porous medium." *Meccanica* 45, no. 6 (2010): 835-846. https://doi.org/10.1007/s11012-010-9292-1

[18] Hayat, T., M. Awais, and S. Asghar. "Radiative effects in a three-dimensional flow of MHD Eyring-Powell fluid." *Journal of the Egyptian Mathematical Society* 21, no. 3 (2013): 379-384. https://doi.org/10.1016/j.joems.2013.02.009

[19] Hayat, T., Masood Khan, and M. Ayub. "Couette and Poiseuille flows of an Oldroyd 6-constant fluid with magnetic field." *Journal of mathematical analysis and applications* 298, no. 1 (2004): 225-244. https://doi.org/10.1016/j.jmaa.2004.05.011

[20] Ganesh, G., and W. Sridhar. "Numerical approach of heat and mass transfer of MHD Casson fluid under radiation over an exponentially permeable stretching sheet with chemical reaction and hall effect." *Frontiers in Heat and Mass Transfer (FHMT)* 16 (2021). https://doi.org/10.5098/hmt.16.5

[21] Shafiq, Anum, Andaç Batur Çolak, Tabassum Naz Sindhu, Qasem M. Al-Mdallal, and T. Abdeljawad. "Estimation of unsteady hydromagnetic Williamson fluid flow in a radiative surface through numerical and artificial neural network modeling." *Scientific Reports* 11, no. 1 (2021): 1-21. https://doi.org/10.1038/s41598-021-93790-9

[22] Shafiq, Anum, Andaç Batur Çolak, and Tabassum Naz Sindhu. "Designing artificial neural network of nanoparticle diameter and solid–fluid interfacial layer on single-walled carbon nanotubes/ethylene glycol nanofluid flow on thin slendering needles." *International Journal for Numerical Methods in Fluids* 93, no. 12 (2021): 3384-3404. https://doi.org/10.1002/fld.5038

[23] Shafiq, Anum, Andaç Batur Çolak, Tabassum Naz Sindhu, and Taseer Muhammad. "Optimization of Darcy-Forchheimer squeezing flow in nonlinear stratified fluid under convective conditions with artificial neural network." *Heat Transfer Research* 53, no. 3 (2022). https://doi.org/10.1615/HeatTransRes.2021041018

[24] Shafiq, Anum, Andaç Batur Çolak, Showkat Ahmad Lone, Tabassum Naz Sindhu, and Taseer Muhammad. "Reliability modeling and analysis of mixture of exponential distributions using artificial neural network." *Mathematical Methods in the Applied Sciences* (2022). https://doi.org/10.1002/mma.8178

[25] Çolak, Andaç Batur, Anum Shafiq, and Tabassum Naz Sindhu. "Modeling of Darcy–Forchheimer bioconvective Powell Eyring nanofluid with artificial neural network." *Chinese Journal of Physics* 77 (2022): 2435-2453. https://doi.org/10.1016/j.cjph.2022.04.004

[26] Shafiq, Anum, Andaç Batur Çolak, and Tabassum Naz Sindhu. "Modeling of Soret and Dufour's convective heat transfer in nanofluid flow through a moving needle with artificial neural network." *Arabian Journal for Science and Engineering* (2022): 1-14. https://doi.org/10.1007/s13369-022-06945-9

[27] Shateyi, S., and S. S. Motsa. "Variable viscosity on magnetohydrodynamic fluid flow and heat transfer over an unsteady stretching surface with Hall effect." *Boundary Value Problems* 2010 (2010): 1-20. https://doi.org/10.1155/2010/257568

[28] Makukula, Z., S. S. Motsa, and P. Sibanda. "On a new solution for the viscoelastic squeezing flow between two parallel plates." *Journal of Advanced Research in Applied Mathematics* 2, no. 4 (2010): 31-38. https://doi.org/10.5373/jaram.455.060310

[29] Ahmed, Mohammed A. Mohammed, Mohammed E. Mohammed, and Ahmed A. Khidir. "On linearization method to MHD boundary layer convective heat transfer with low pressure gradient." *Propulsion and Power Research* 4, no. 2 (2015): 105-113. https://doi.org/10.1016/j.jppr.2015.04.001

[30] Salah, Faisal, A. K. Alzahrani, Abdelmgid OM Sidahmed, and K. K. Viswanathan. "A note on thin-film flow of Eyring-Powell fluid on the vertically moving belt using successive linearization method." *International Journal Of Advanced And Applied Sciences* 6, no. 2 (2019): 17-22. https://doi.org/10.21833/ijaas.2019.02.004

[31] Reddy, Nalivela Nagi, Vempati Srinivasa Rao, and B. Ravindra Reddy. "Chemical reaction impact on MHD natural convection flow through porous medium past an exponentially stretching sheet in presence of heat source/sink and viscous dissipation." *Case studies in thermal engineering* 25 (2021): 100879. https://doi.org/10.1016/j.csite.2021.100879

[32] Khalili, Noran Nur Wahida, Abdul Aziz Samson, Ahmad Sukri Abdul Aziz, and Zaileha Md Ali. "Chemical reaction and radiation effects on MHD flow past an exponentially stretching sheet with heat sink." In *Journal of Physics: Conference Series*, vol. 890, no. 1, p. 012025. IOP Publishing, 2017. https://doi.org/10.1088/1742-6596/890/1/012025

[33] Fetecau, C., Sharat C. Prasad, and K. R. Rajagopal. "A note on the flow induced by a constantly accelerating plate in an Oldroyd-B fluid." *Applied mathematical modelling* 31, no. 4 (2007): 647-654. https://doi.org/10.1016/j.apm.2005.11.032

[34] Hayat, T., M. Imtiaz, and A. Alsaedi. "Boundary layer flow of Oldroyd-B fluid by exponentially stretching sheet." *Applied Mathematics and Mechanics* 37, no. 5 (2016): 573-582. https://doi.org/10.1007/s10483-016-2072-8

[35] Sparrow, E. M., and J. P. Abraham. "A new buoyancy model replacing the standard pseudo-density difference for internal natural convection in gases." *International Journal of Heat and Mass Transfer* 46, no. 19 (2003): 3583-3591. https://doi.org/10.1016/S0017-9310(03)00152-2

[36] Mukhopadhyay, Swati. "MHD boundary layer flow and heat transfer over an exponentially stretching sheet embedded in a thermally stratified medium." *Alexandria Engineering Journal* 52, no. 3 (2013): 259-265. https://doi.org/10.1016/j.aej.2013.02.003

[37] Swain, I., S. R. Mishra, and H. B. Pattanayak. "Flow over exponentially stretching sheet through porous medium with heat source/sink." *Journal of Engineering* 2015 (2015). https://doi.org/10.1155/2015/452592